sustainability

MDPI

Article

Characterization and Sustainability Potential of Recycling 3D-Printed Nylon Composite Wastes

Noura Al-Mazrouei [1], Ali H. Al-Marzouqi [1] and Waleed Ahmed [2,*]

[1] Chemical and Petroleum Engineering Department, UAE University, Al-Ain P.O. Box 15551, United Arab Emirates
[2] Engineering Requirements Unit, UAE University, Al-Ain P.O. Box 15551, United Arab Emirates
* Correspondence: w.ahmed@uaeu.ac.ae

Abstract: The revolution of 3D-printing technology has caused an additional source of plastic waste, especially the new generation of composite filaments that are linked with the commercial fused deposition modeling process, adding pressure to find a sustainable solution to tackle the emerging waste problem. This study aims to investigate the mechanical and thermal properties of a blended recycled composite material produced by mixing two different 3D-printed reinforced composite wastes, carbon fiber CF/nylon, and glass fiber GF/nylon filaments that were mixed at different percentages using a hot extrusion procedure, tested by a tensile testing machine, and processed with five different weight ratios to study the impact of blend ratios on the material characteristics of the recycled composites and to find the optimum weight ratios with the most preferred properties. The results revealed that the maximum tensile strength of the GF/nylon composite was achieved with 60 wt%. The highest elastic modulus value was recorded at 60 wt% GF/nylon. Moreover, it was noted that at 80 wt% of GF/nylon, the ductility is at the peak value among the composites.

Keywords: sustainability; recycling; 3D printed; nylon; composite wastes

Citation: Al-Mazrouei, N.; Al-Marzouqi, A.H.; Ahmed, W. Characterization and Sustainability Potential of Recycling 3D-Printed Nylon Composite Wastes. *Sustainability* **2022**, *14*, 10458. https://doi.org/10.3390/su141710458

Academic Editors: Manfredi Saeli and David Maria Tobaldi

Received: 24 July 2022
Accepted: 17 August 2022
Published: 23 August 2022

1. Introduction

The increased production and use of plastics and reinforced fibers have numerous damaging environmental impacts [1]. According to a published report in 2016, it is anticipated that by 2050, the world's oceans will have more plastic waste than fish [2]. There are many plastics, such as polyethylene (PET), high-density polyethylene (HDPE), polyvinyl chloride (PVC), and many others that are used for daily purposes and are disposed of in landfills [3]. As the world population continues expanding, the demand for consumables will increase. The revolution of 3D-printing technology, known as additive manufacturing (AM), has been developed to boost the industrial sector in producing models, prototypes, jigs and fixtures, and spare parts for various manufacturing processes. There are many reasons to produce 3D-printed plastic wastes using the FDM 3D-printing technology, such as waste prints due to low-quality filament, bed adhesion issues, hardware failures, and slicing errors. Recycling has always been one of the most preferred solutions to addressing and handling the problem of plastic waste [4]. Usually, recycling polymers, such as carbon fiber and glass fiber, are not accessible due to toxic heavy metals that are produced during the process. However, during the manufacturing process of carbon fiber, 30% of waste can be recycled [5,6]. In the case of AM processes, such as FDM 3D-printing technology, waste of the 3D-printed objects can be recycled and reused again since most of the 3D-printed parts are used for prototyping. The main concern with recycling 3D-printed waste is the challenge of dimensional quality control and material properties consistency [7]. Regarding the other 3D-printed wastes, more environment-friendly polymer processes should be developed through sustainable methods in the case of different thermoplastic polymers, such as polyethylene, polypropylene, polyvinyl chloride, and nylon [8]. Over

the last two decades, AM has become an invaluable tool with applications in making models, prototypes, and mold inserts in manufacturing methods. AM can be used in many fields, from arts, medicine, and car manufacturing to engineering [9–14]. Because of the development of low-cost polymer additive manufacturing, the industry is developing incredibly fast [15,16]. The common processes of 3D-printing technology are fused deposition modeling (FDM), stereolithography (SLA), and selective laser sintering (SLS) [17,18]. In addition, the technology has taken the lead in manufacturing sustainability by reducing the environmental impact [19–22]. AM will play a crucial role in revolutionizing the future industry as most industries have adopted this technology for various applications. Fused filament fabrication (FFF), also known as fused deposition modeling (FDM), is an additive manufacturing technology based on material extrusion. This technique can be simulated as a standard plastic extruder in which the material is pushed into the printing head, melts, and is extruded out through a nozzle to produce a thin filament instead of using injection molds [23]. The widely used polymer materials in FDM are acrylonitrile butadiene styrene (ABS), polylactic acid (PLA), and polycarbonate (PC) [24,25], but the most dominant is the biodegradable material, PLA. For manufacturing purposes, synthetic polymers are desirable due to their properties, including plastics, nylons, and polyesters. Thermoplastic polymers have better physical properties than other polymers, which make them ideal for additive manufacturing as they are recyclable and easy to mold into various shapes. Common thermoplastics used in injection molding include acrylonitrile butadiene styrene (ABS), polylactic acid (PLA), polycarbonate (PC), and nylon (polyamide 12) for mass production [26,27]. Thermoplastic polymers are further used in fabricating pipes, ropes, belts, and insulators. The 3D-printed parts of polymers has emerged with increased research leading to increased use of polymers in various industries [28,29]. Polymer printing is preferred for low massive production and prototyping as it is cost-effective, and functional parts with distinct capabilities and properties can be printed. Some standard polymeric 3D-printed materials include ABS, PLA, and nylon [30]. In engineering plastic applications, nylon is preferred due to its versatility in transforming into fibers, films, and molded parts known as polyamide. As nylon is a thermoplastic polymer that can quickly be melted, it can be printed using either the FDM or the SLS process [31–33]. The post-use of the produced plastic waste has numerous unfavorable impacts on the environment when not properly managed [20,34]. According to the published literature, nylon reinforcement with fibers can improve its machinal and thermal characteristics. Wang et al. published a study about glass-fiber-reinforced nylon (GF/PA), and it has been observed that mechanical properties are enhanced due to the addition of fibers [31,35]. Carbon fiber-reinforced nylon (CFRN) filament was developed as a printable polymer composite due to its high performance. Carbon-fiber-reinforced plastics (CFRPs) are desired among conventional thermoplastics since they have superior mechanical properties [36]. A study investigating the properties of 3D parts produced from CFRPs found they have better impact strength along with high resistance to greases, oils, fuels, water, alkalis, and salt [37]. When using polyamide (PA) as a matrix, the mechanical properties are affected by the moisture-sensitive nature of the matrix [38]. CFRPs have applications in manufacturing engineering parts, custom end-use production parts, structural parts, fixtures, jigs prototyping, testing, and other tooling equipment [37]. The main challenge of using CFRPs is to ensure the production of CFRPs with good consolidation of reinforcement in the polymer structure [39,40]. However, it has been reported that the characteristics of materials reinforced with nylon (PA6) are enhanced with the addition of glass fiber (GF) [41]. Unfortunately, 100 wt% nylon has a significantly lower elastic modulus and yield compared to a composite with 80% nylon and 20% GF [42,43]. Glass fibers have superior properties, including high toughness and ductility, rigidity, and resistance to chemical deterioration. Various technologies can be used to prepare GF-reinforced fibers. Another study investigated the use of fiber-reinforced ABS manufactured using FDM [44]. Glass fiber was added to increase material strength but reduced the flexibility of the resulting material. The advantages of using GF-reinforced ny-

lons include having a high softening point, low friction coefficient, good shock absorption, good electrical insulation, and is odorless and weather resistant [45].

In this study, composite waste of 3D-printing technology, the CF/nylon, and GF/nylon were blended at different concentrations to produce recycled CFGF/nylon composite sheets and were tested for their mechanical and thermal properties. Both materials' filaments were collected from 3D-printed waste resources. The composite sheets were subjected to different tests to examine their mechanical properties, such as tensile strength, elasticity modulus, ductility, toughness, and thermal properties.

2. Material and Methods

Two 3D-printed composite wastes were used in this investigation: nylon-carbon fiber filament (CF/nylon) and nylon-glass fiber filament (GF/nylon). CF/nylon filament is made of nylon matrix with approximately 20% carbon fiber (CF), and GF/nylon filament is made from nylon matrix and 16% of glass fiber reinforcement, according to the fiber force filaments supplier [46,47]. However, the 3D-printing material waste was collected from the prototyping laboratories and recycled material using a robust shredding machine with stainless steel blades to break it down into small pieces. Furthermore, the material that was gathered from the shredding device was also broken down into smaller pieces using a heavy-duty mixer designed explicitly for hardwood until no shredder residues were found. The shredded materials were small enough to fit into the extruder feed hopper and had an estimated length of 10 mm.

Five different mixing ratios and two pure materials, i.e., nylon carbon fiber and nylon glass fiber, were studied, as illustrated in Table 1.

Table 1. Weight percentages of composite samples.

Samples	CF/nylon, wt%	GF/nylon, wt%
CF/nylon	100	0
Blend 1	80	20
Blend 2	60	40
Blend 3	50	50
Blend 4	40	60
Blend 5	20	80
GF/nylon	0	100

CF/nylon and GF/nylon were mixed in ratios based on the planned percentages required to develop composite materials. The samples were extruded using a twin-screw extruder (MiniLab H.A.A.K.E. Rheomex CTW5, Karlsruhe, Germany). Each set of composites and two pure materials were operated in a control system for 5 min at 250 °C and 70 r/min screw rotation to maintain the ideal mixing characteristics. During the material preparation process, a twin extruder was utilized to mix and push out the material via a valve to collect the product for use at a later stage in the manufacturing process, as shown in Figure 1. A Carver's hot press (CarverTM lab presses) was used to compress the extruded composites for 5 min at 250 °C and 35 MPa pressure to produce a thin layer of composite sheets for testing the mechanical properties.

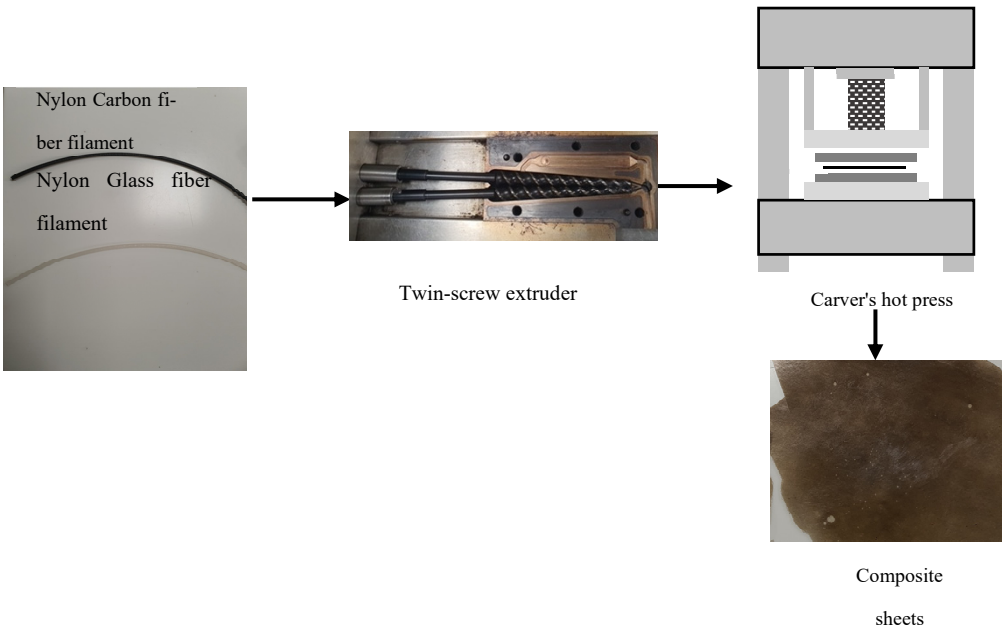

Figure 1. Schematic diagram of the material preparation process.

A universal testing machine (UTM, Shimadzu) was used to test the composite sheets for the mechanical properties formed from the mixtures of CF/nylon and GF/nylon. A customized manual blanking machine was used to produce the samples for the tensile test (Exacta Model-JFP) [48,49]. The sheets produced were tested under tensile load conditions following ASTMD-638. Moreover, Figure 2 presents the measurements of the sample, as specified by the standard ASTMD-638.

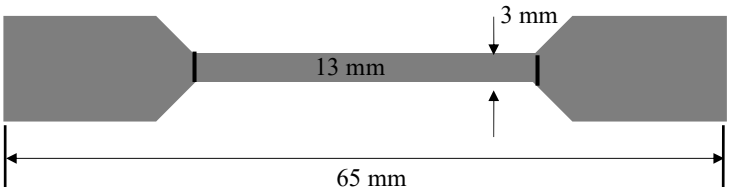

Figure 2. Sample dimensions.

Mechanical strength is becoming more important as the usage of plastics continues to rise. The tested composite sheets were made in a dog bone shape, but for pure GF/nylon, the 80 and 60 wt% GF/nylon measured 13 (L) × 3 (W) × 0.21 mm (thickness), while for pure CF/nylon, 20, 40, and 50 wt% of GF/nylon, the composite sheets were 13 (L) × 3 (W) × 0.25 mm (thickness). Reinforced polymers were tested according to ASTM D-882 to determine their tensile characteristics, as shown in Figure 3. As part of ASTM D-882 the specimen was subjected to tensile stress, while different specimen parameters were measured. The test was carried out at a speed of 5 mm/min on a universal testing machine until the specimen failed. Various kinds of plastics are subject to a wide range of testing procedures, but according to ASTMD-882 it is only applicable to samples of hard plastic with a thickness less than 1.00 mm [50–53].

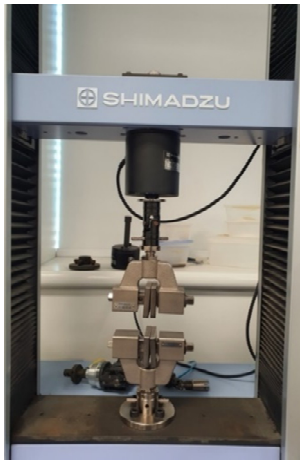

Figure 3. Tensile testing machine.

The mechanical characteristics of the prepared samples were evaluated according to ASTMD-638 standard. The average results of seven tested composite samples were used while calculating the mechanical properties. A specimen's tensile strength was calculated using Equation (1) [54].

$$\text{Tensile Strength (Pa)} = \frac{\text{Maximum load measured (N)}}{\text{Gauge length original area (m}^2\text{)}} \quad (1)$$

According to the consistency of deformation of the gauge length of the sample, elongation values were validated. Further, it was statistically significant and acceptable to use in engineering design applications. During the tensile testing, this specimen undergoes non-uniform deformation (necking), which facilitates measuring the nominal strain within the required gauge length. Prolongation (i.e., change in gage length) was calculated using Equation (2) [54].

$$\text{Ductility} = \frac{L_f - L_0}{L_0} \times 100 \quad (2)$$

where:

L_f = ruptured specimen length, and L_0 = original length.

From Equation (3), the elastic modulus was calculated in which the gauge length segment was considered as the average cross-sectional area (A_c) of the sample. The A_c was obtained from the average cross-sectional area of the selected samples [55]. For samples with no evidence of proportionality, the secant values were computed. Those values were obtained by projecting a tangent that passes across zero stress.

$$E = \frac{\Delta\sigma(\varepsilon)}{\Delta\varepsilon} = \frac{F/A}{\Delta L/\, L_0} = \frac{F \cdot L_0}{A \cdot \Delta L} \quad (3)$$

where:

E = elasticity modulus,
F = tension force,
A = actual cross-sectional area,
ΔL = change in length, and
L_0 = sample original length.

Toughness is defined as the area under the curve obtained from the stress–strain graph, which was calculated using Equation (4) [56].

$$\text{Toughness} = \text{area under the stress-strain curve} \quad (4)$$

3. Results and Discussion

The mechanical properties of CFGF/nylon, consisting of CF/nylon with various ratios of GF/nylon were estimated from the mechanical tensile test. According to the fiber force company in Italy, for 3D-printed filament, pure CF/nylon tensile strength is 66.3 MPa with an elastic modulus and ductility of 2758 MPa and 6.7%, respectively. On the other hand, pure GF/nylon tensile strength is 64.7 MPa, the elastic modulus is 2534 MPa, and ductility is 9.2% [57,58]. The composite blend samples determined other properties, such as toughness, tensile strength, yield strength, elastic modulus, and ductility. The samples were molded into dog-bone sheets, which were used to conduct repeated tensile tests of the materials under examination. The Mitutoyo thickness gage of model 547-526S was utilized to calculate the film thickness due to its high resolution of 0.001 mm [59]. In this research, the mechanical properties values for all seven samples were recorded.

Pure CF/nylon and GF/nylon have been used as standards to compare the effects of variations in the composition and pure samples in the current study [54]. Figure 4 depicts that at 100 wt% CF/nylon has a tensile strength of 64 MPa. By adding a 20% GF/nylon weight to CF/nylon the tensile strength increases by 2%, and another 20 wt% addition increases it by another 2%. The tensile strength steadily rose to 67 MPa at 50 wt% GF/nylon and 68 MPa at 60 wt% GF/nylon, reaching its peak. This means that the GF/nylon content increases the adhesion between both materials and generates higher strength. An increase in GF/nylon composition after this point reduced the tensile strength. Tensile strength is 12% lower at 80 wt% GF/nylon than at 60 wt% GF/nylon. A drop in tensile strength to 59 MPa was observed as it reached 100 wt% of GF/nylon. It is worth mentioning that GF/nylon has the lowest tensile strength at 100 wt%, even when compared to pure CF/nylon. Based on Güllüa et al.'s studies, the varying tensile strength values are obtained due to many factors. During the extruding process, the temperature might decrease, which can affect the sample and cause some crystallinity, and depending on the crystalline level, the fracture area may vary, which requires extra stress in case of high-crystalline degree.

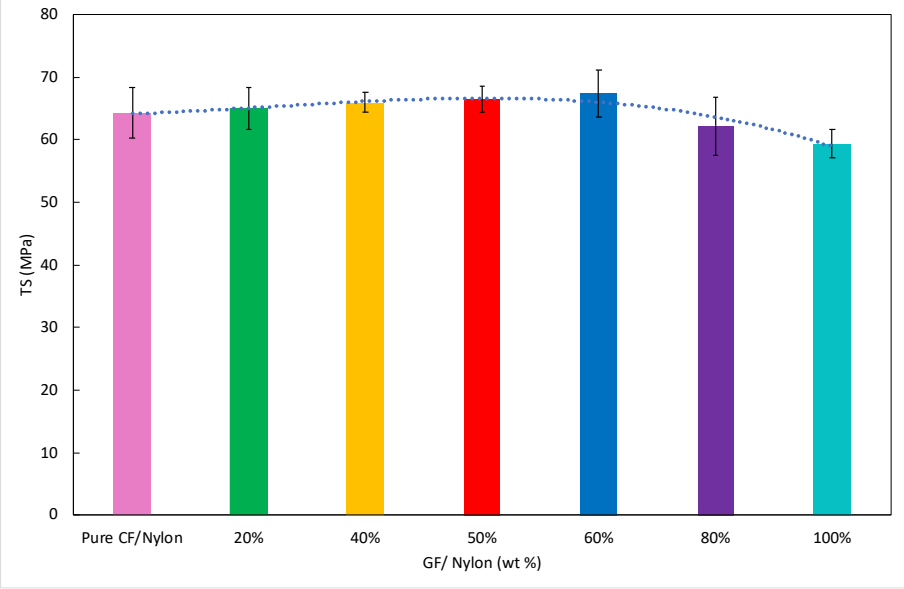

Figure 4. Comparison of tensile strength of the composites.

While studying the mechanical properties of any component, determining and using the elastic modulus is essential [60]. As illustrated in Figure 5 pure CF/nylon has an elastic modulus of 2740 MPa. Adding 20 wt% of GF/nylon into the CF/nylon increased the elastic modulus by 4.5%, and another 20 wt% addition further increased it by 6%. The elastic modulus steadily rises to 3361 MPa at 50 wt% GF/nylon and 3430 MPa at 60 wt% of GF/nylon. This means that when the weight of the GF/nylon composite is increased,

inelastic deformation occurs. Therefore, the increased content of GF/nylon in the nylon composite shows significant improvement in the elasticity of the composite. A further increase in GF/nylon at 80 wt% decreased the elastic modulus by 7.5%. It has also been reported that the formation of voids in specimens might occur during mixing. A significant degree of plastic deformation will be discovered in methods that detect voids and particle aggregation [61].

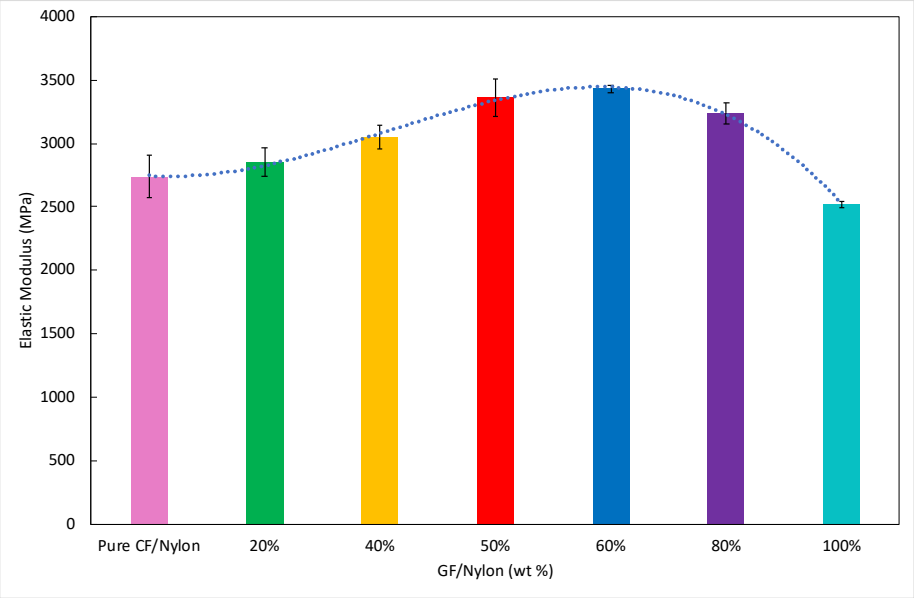

Figure 5. Comparison of elastic modulus of the composites.

The term "ductility" is the ability of a material to undergo permanent deformation, for example, stretch, bend, or spread in reaction to stress. It is a mechanical attribute typically referred to as a material's ability to be drawn into a wire [62,63]. The paper published by Chong et al. states that recycled 3D-printed polymers, high-density polyethylene (HDPE), and polypropylene (PP) combined with varying concentrations of activated carbon show an enhanced ductility that would, in turn, be helpful in the process of 3D-printed items with more excellent elasticity [64–66]. It can be seen in Figure 6 that pure GF/nylon demonstrated a ductility percentage of 8.9%, but pure CF/nylon showed 6.8% ductility. The further addition of 20 wt% of GF/nylon to CF/nylon, increased the ductility by 1%. This means that the ductility percentage of pure CF/nylon is similar to the 40 wt% of GF/nylon. The ductility percentage steadily dropped to 6.5% at 50 wt% GF/nylon and 6.2% at 60 wt% GF/nylon, meaning that it is at its most brittle state and can fracture very easily under a tensile load. There is a sharp increase to 7.8% ductility at 80 wt% GF/nylon.

Toughness is described as the resistance of a substance to fracture when stress is applied. Toughness necessitates a delicate balance of strength and ductility [67]. In this study, pure CF/nylon was used as a reference to compare the variation of the glass composition in nylon with its respective toughness. The results in Figure 7 show that pure CF/nylon has a toughness of 11.50 MPa. The toughness is then increased by 6% after adding 20 wt% of GF/nylon and up to 4% by adding another 20 wt% GF/nylon. There is a slight increase of 1% in toughness at 50 wt% GF/nylon. The toughness rate at 60 wt% of GF/nylon is 14 MPa and 15 MPa at 80 wt%. It has the highest toughness rate of 16.53 MPa at 100 wt% of GF/nylon. Recycling of polyamide 12 (PA12) filament was the primary focus of the Vidakis et al. research. According to their findings, the mechanical and thermal stability of the recycled 3D-printed filament improved compared to the original filaments [68,69]. The detailed results of the mechanical properties are shown in Table 2.

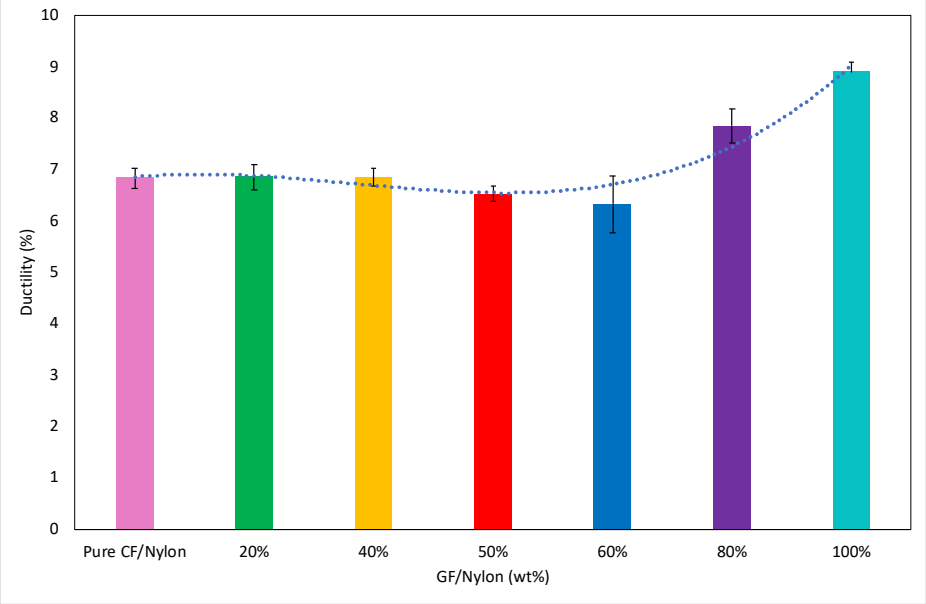

Figure 6. Comparison of ductility of the composites.

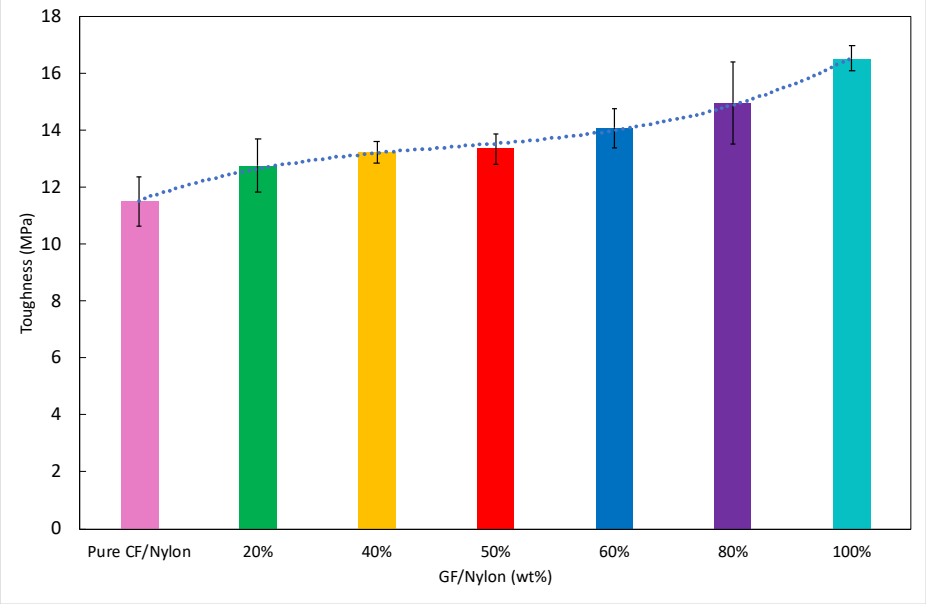

Figure 7. Comparison of the toughness of the composites.

Table 2. The mechanical properties of the CFGF/nylon composites with standard deviation (SD).

GF/Nylon (%)	Tensile Strength (MPa)	SD	Ductility (%)	SD	Elastic Modulus (MPa)	SD	Toughness (MPa)	SD
Pure CF/Nylon	64.20	±4.07	6.83	±0.20	2740.23	±170.81	11.50	±0.88
20%	64.90	±3.35	6.86	±0.25	2850.70	±113.99	12.76	±0.93
40%	65.90	±1.63	6.85	±0.17	3050.67	±97.11	13.24	±0.39
50%	66.40	±2.10	6.53	±0.15	3360.84	±148.13	13.35	±0.54
60%	67.40	±3.69	6.33	±0.55	3430.08	±32.77	14.08	±0.69
80%	62.20	±4.62	7.86	±0.34	3240.50	±81.63	14.97	±1.45
100%	59.30	±2.27	8.90	±0.20	2520.01	±23.26	16.54	±0.46

4. Thermogravimetric Analysis (TGA)

Thermogravimetric analysis (TGA) is essential for studying elastomers' thermal behavior. TGA involves continuous monitoring of the weight of a sample while the temperature is increased continuously. A loss in weight is observed when the sample degrades since decomposition components vaporize [70,71]. From the acquired TGA data, the percentage mass loss was calculated by dividing the final weight at each particular temperature by the initial mass of the sample taken for the experiments.

As shown in Figure 8 GF/nylon degrades relatively at a lower temperature than pure CF/nylon, indicating less stability for GF/nylon than CF/nylon. The pure sample in GF/nylon starts to degrade at 397 °C up to 474 °C. However, in pure CF/nylon, the degradation starts at 414 °C and continues to 490 °C. In both pure GF/nylon and CF/nylon, the percentage of weight loss after degradation remains the same, which is 92%. The inference from the above observation is that CF/nylon has better thermal properties [72].

All CFGF/nylon samples were thermally stable up to 403 °C. However, there were minor differences in the tested samples. As more GF/nylon was added to the sample, the material's thermal stability increased slightly. Over 90% of the material was degraded in all composite samples, causing weight loss starting from 422 °C to 489 °C. The threshold decomposition temperature indicates the highest processing temperature that can be adopted [73,74].

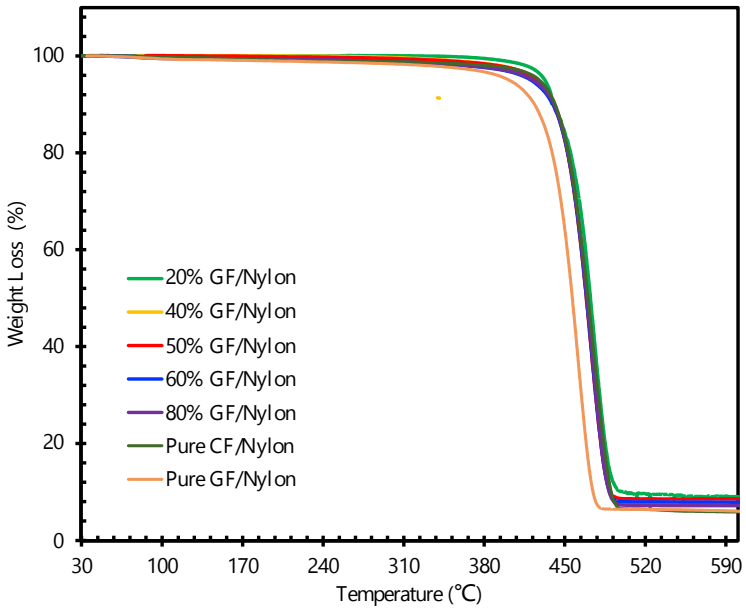

Figure 8. TGA results for pure and different compositions of GF/nylon.

5. Fourier Transform Infrared (FTIR) Spectroscopy

The Fourier transform infrared (FTIR) spectroscopy was used to identify constituents of organic substances and functional groups. The specimens are subjected to infrared (IR) radiation for an extended time to obtain FTIR results. Because the infrared radiations act on the atomic oscillation of the particle in the specimen, a specific kind of energy absorption or transmission may be observed [75,76].

FTIR spectra of pure CF/nylon and pure GF/nylon samples are given in Figure 9. Since all composites tested to contain a high percentage of nylon, the FTIR results show a similar functional group. The peaks included a single bond area (2500–3500 cm^{-1}). As shown in Figure 9 there is an intense bond at about 3283 cm^{-1}, indicating the existence of N-H stretching from the amino group. Around 2850 cm^{-1} and 2920 cm^{-1}, the intensity between pure GF/nylon and CF/nylon was noticed, but the existing group for both peaks is CH_2 asymmetric stretching. A narrow bond at less than 1000 cm^{-1} represented the C-H bond [77].

The spectrum of prepared composites reveals differences in intensities. Vibrations of N-H stretching (3284 cm^{-1}) show a slight absorption difference in both composites. Even with slight varying peaks in all composites, the wavelengths of (2848 cm^{-1}) and (2916 cm^{-1}) show C-H stretching due to the alkanes group. The peaks in the range of 1500–1700 cm^{-1} show the presence of amide I and II bands, in this case, 1631.97 cm^{-1} and 1550 cm^{-1}. This group has an active hydrogen group and contributes to cross-linking formation [78,79].

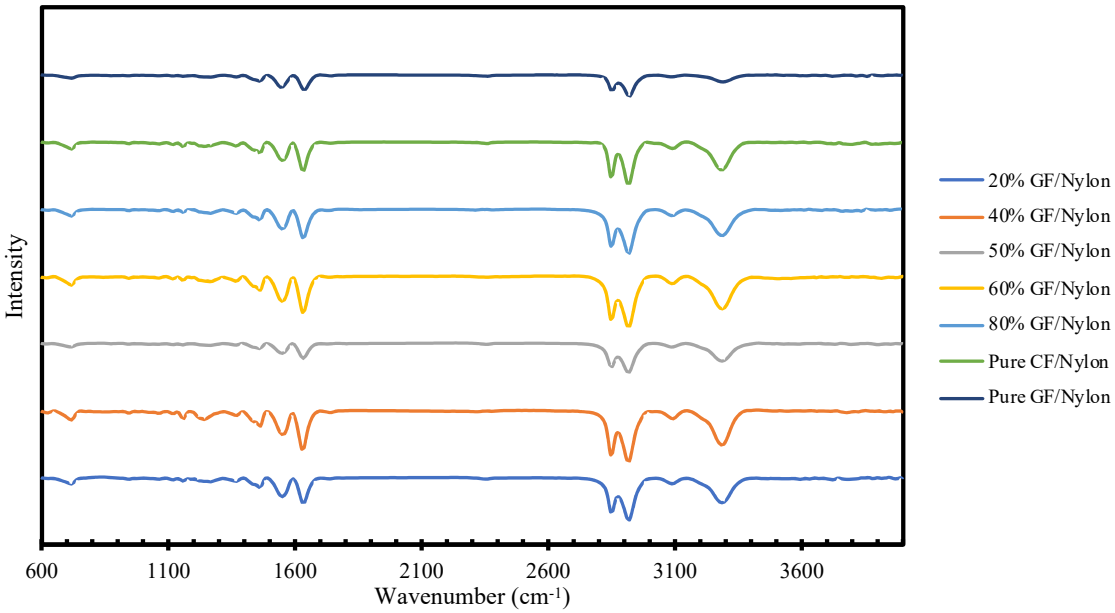

Figure 9. FT-IR results for pure and different compositions of GF/nylon.

6. Conclusions

AM, also referred to as three-dimensional (3D)-printing technology, is a technique for fast prototyping that can be used for various types of materials. Furthermore, recycling wastes produced from 3D-printed objects and 3D components after they have reached the end of their lifespans is a fundamental problem that must be addressed [80].

This study combined a compression molding process with a twin extruder machine to manufacture composite sheets by varying compositions of CF/nylon and GF/nylon. The mechanical analysis of the processed composites revealed an increase in tensile strength of CF/nylon to 65 MPa when 20 wt% of GF/nylon was added. But the ductility and toughness of the composites recorded the highest values in pure GF/nylon (8.9% and 16.25 MPa, respectively). When the ratio of GF/nylon was increased from 50 wt% to 60 wt%, the maximum elastic modulus increased from 3361 MPa to 3430 MPa. On the other hand, the elastic modulus decreased slightly, falling to 3240 MPa at a weight of 80 wt% GF/nylon. On the other hand, in TGA results, pure CF/nylon has a higher degradation temperature than pure GF/nylon. Additionally, when adding GF/nylon, the degradation temperature decreased.

The biodegradability of 3D-printed filaments is a topic of active study. Many research efforts are being aimed toward improving biobased 3D-printed filaments. This study can be extended to further research in recycling different materials of 3D-filament waste.

Author Contributions: Conceptualization, A.H.A.-M.; Data curation, A.H.A.-M.; Formal analysis, N.A.-M. and W.A.; Funding acquisition, W.A.; Investigation, N.A.-M. and W.A.; Methodology, W.A.; Project administration, A.H.A.-M.; Software, N.A.-M.; Validation, A.H.A.-M.; Writing—original draft, N.A.-M. All authors have read and agreed to the published version of the manuscript.

Funding: This research and APC were funded by UAE University, Grant number G00003334.

Institutional Review Board Statement: Not applicable.

Informed Consent Statement: Not applicable.

Data Availability Statement: Not applicable.

Conflicts of Interest: The authors declare no conflict of interest.

References

1. Suksiripattanapong, C.; Phetprapai, T.; Singsang, W.; Phetchuay, C.; Thumrongvut, J.; Tabyang, W. Utilization of Recycled Plastic Waste in Fiber Reinforced Concrete for Eco-Friendly Footpath and Pavement Applications. *Sustainability* **2022**, *14*, 6839. [CrossRef]
2. Nizamuddin, S.; Boom, Y.J.; Giustozzi, F. Sustainable polymers from recycled waste plastics and their virgin counterparts as bitumen modifiers: A comprehensive review. *Polymers* **2021**, *13*, 3242. [CrossRef] [PubMed]
3. Alhazmi, H.; Almansour, F.H.; Aldhafeeri, Z. Plastic waste management: A review of existing life cycle assessment studies. *Sustainability* **2021**, *13*, 5340. [CrossRef]
4. Abdissa, G.; Ayalew, A.; Dunay, A.; Illés, C.B. Role of Reverse Logistics Activities in the Recycling of Used Plastic Bottled Water Waste Management. *Sustainability* **2022**, *14*, 7650. [CrossRef]
5. Holmes, M. Recycled carbon fiber composites become a reality. *Reinf. Plast.* **2018**, *62*, 148–153. [CrossRef]
6. Karuppannan Gopalraj, S.; Kärki, T. A review on the recycling of waste carbon fibre/glass fibre-reinforced composites: Fibre recovery, properties and life-cycle analysis. *SN Appl. Sci.* **2020**, *2*, 433. [CrossRef]
7. Taylor, S. *Waste Management Implications of 3D Printing*; EcoMENA: Doha, Qatar, 2014.
8. Epps, T.H., III; Korley, L.T.; Yan, T.; Beers, K.L.; Burt, T.M. Sustainability of Synthetic Plastics: Considerations in Materials Life-Cycle Management. *JACS Au* **2021**, *2*, 3–11. [CrossRef]
9. Gebhardt, A. *Understanding Additive Manufacturing*; Elsevier: Amsterdam, The Netherlands, 2011. [CrossRef]
10. Jang, G.-E.; Cho, G.-Y. Effects of Ag Current Collecting Layer Fabricated by Sputter for 3D-Printed Polymer Bipolar Plate of Ultra-Light Polymer Electrolyte Membrane Fuel Cells. *Sustainability* **2022**, *14*, 2997. [CrossRef]
11. Wohlers, T.; Gornet, T. History of additive manufacturing. *Wohlers Rep.* **2014**, *24*, 118.
12. Wong, K.; Hernandez, A. A Review of Additive Manufacturing. *Int. Sch. Res. Netw.* **2012**, *2012*, 208760. [CrossRef]
13. Sun, H.; Zheng, H.; Sun, X.; Li, W. Customized Investment Decisions for New and Remanufactured Products Supply Chain Based on 3D Printing Technology. *Sustainability* **2022**, *14*, 2502. [CrossRef]
14. Stansbury, J.; Idacavage, M. 3D printing with polymers: Challenges among expanding options and opportunities. *Dent. Mater.* **2016**, *32*, 24–64. [CrossRef] [PubMed]
15. Love, L.; Kunc, V.; Rios, O.; Duty, C.; Elliott, A.; Post, B.; Smith, R.; Blue, C. The importance of carbon fiber to polymer additive manufacturing. *J. Mater. Res.* **2014**, *29*, 1893–1898. [CrossRef]
16. Guo, N.; Leu, M. Additive manufacturing: Technology, applications and research needs. *Front. Mech. Eng.* **2013**, *8*, 215–243. [CrossRef]
17. Pilipović, A.; Ilinčić, P.; Bakić, A.; Kodvanj, J. Influence of Atmospheric Conditions on Mechanical Properties of Polyamide with Different Content of Recycled Material in Selective Laser Sintering. *Polymers* **2022**, *14*, 2355. [CrossRef]
18. Mahamood, R.M.; Akinlabi, S.A.; Shatalov, M.; Murashkin, E.V.; Akinlabi, E.T. Additive Manufacturing/3D Printing Technology: A Review. *Ann. Dunarea Jos Univ. Galati. Fascicle XII Weld. Equip. Technol.* **2019**, *30*, 51–58. [CrossRef]
19. Al-Sinan, M.A.; Bubshait, A.A. Using Plastic Sand as a Construction Material toward a Circular Economy: A Review. *Sustainability* **2022**, *14*, 6446. [CrossRef]
20. Immonen, K.; Metsä-Kortelainen, S.; Nurmio, J.; Tribot, A.; Turpeinen, T.; Mikkelson, A.; Kalpio, T.; Kaukoniemi, O.-V.; Kangas, H. Recycling of 3D Printable Thermoplastic Cellulose-Composite. *Sustainability* **2022**, *14*, 2734. [CrossRef]
21. Abdulhameed, O.; Al-Ahmari, A.; Ameen, W. Additive manufacturing: Challenges, trends, and applications. *Adv. Mech. Eng.* **2019**, *11*, 1–27. [CrossRef]
22. Ahmad, A.; Darmoul, S.; Ameen, W.; Abidi, M.; Al-ahmari, A. Rapid Prototyping for Assembly Training and Validation. *Int. Fed. Autom. Control* **2015**, *48*, 412–417. [CrossRef]
23. Williams, C.; Mistree, F.; Rosen, D. A Functional Classification Framework for the Conceptual Design of Additive Manufacturing Technologies. *J. Mech. Des.* **2011**, *133*, 121002. [CrossRef]
24. Karayannis, P.; Saliakas, S.; Kokkinopoulos, I.; Damilos, S.; Koumoulos, E.P.; Gkartzou, E.; Gomez, J.; Charitidis, C. Facilitating Safe FFF 3D Printing: A Prototype Material Case Study. *Sustainability* **2022**, *14*, 3046. [CrossRef]
25. Lee, C.H.; Padzil, F.N.B.M.; Lee, S.H.; Ainun, Z.M.A.A.; Abdullah, L.C. Potential for natural fiber reinforcement in P.L.A. polymer filaments for fused deposition modeling (FDM) additive manufacturing: A review. *Polymers* **2021**, *13*, 1407. [CrossRef]
26. Arefin, A.; Khatri, N.; Kulkarni, N.; Egan, P. Polymer 3D Printing Review: Materials, Process, and Design Strategies for Medical Applications. *Appl. 3D Print. Polym.* **2021**, *13*, 1499. [CrossRef]
27. Khaki, S.; Rio, M.; Marin, P. Characterization of Emissions in Fab Labs: An Additive Manufacturing Environment Issue. *Sustainability* **2022**, *14*, 2900. [CrossRef]
28. Connor, H.; Dowling, D. Comparison between the properties of polyamide 12 and glass bead filled polyamide 12 using the multi jet fusion printing process. *Addit. Manuf.* **2020**, *31*, 100961. [CrossRef]

29. Xu, J.; Zhu, N.; Yang, R.; Yang, C.; Wu, P. Effects of Extracellular Polymeric Substances and Specific Compositions on Enhancement of Copper Bioleaching Efficiency from Waste Printed Circuit Boards. *Sustainability* **2022**, *14*, 2503. [CrossRef]
30. Song, X.; He, W.; Qin, H.; Yang, S.; Wen, S. Fused Deposition Modeling of Poly (lactic acid)/Macadamia Composites—Thermal, Mechanical Properties and Scaffolds. *Materials* **2020**, *13*, 258. [CrossRef]
31. Shakiba, M.; Rezvani Ghomi, E.; Khosravi, F.; Jouybar, S.; Bigham, A.; Zare, M.; Ramakrishna, S. Nylon—A material introduction and overview for biomedical. *Polym. Adv. Technol.* **2021**, *32*, 3368–3383. [CrossRef]
32. Mostafa, K.; Montemagno, C.; Qureshi, A. Strength to cost ratio analysis of FDM Nylon 12 3D Printed Parts. *Procedia Manuf.* **2018**, *26*, 753–762. [CrossRef]
33. Thomas, D. 3D printing durable patient specific knee implants. *J. Orthop.* **2017**, *14*, 182–183. [CrossRef] [PubMed]
34. Jacobs, C.; Soulliere, K.; Sawyer-Beaulieu, S.; Sabzwari, A.; Tam, E. Challenges to the Circular Economy: Recovering Wastes from Simple versus Complex Products. *Sustainability* **2022**, *14*, 2576. [CrossRef]
35. Wang, X.; Wu, G.; Xie, P.; Gao, X.; Yang, W. Microstructure and properties of glass fiber-reinforced polyamide/nylon microcellular foamed composites. *Polymers* **2020**, *12*, 2368. [CrossRef] [PubMed]
36. Pizzorni, M.; Parmiggiani, A.; Prato, M. Adhesive bonding of a mixed short and continuous carbon-fiber-reinforced Nylon-6 composite made via fused filament fabrication. *Int. J. Adhes. Adhes.* **2021**, *107*, 102856. [CrossRef]
37. F Calignano, F.; Lorusso, M.; Roppolo, I.; Minetola, P. Investigation of the mechanical properties of a carbon fibre-reinforced nylon filament for 3D printing. *Machines* **2020**, *8*, 52. [CrossRef]
38. Kikuchi, B.C.; Bussamra, F.L.D.S.; Donadon, M.V.; Ferreira, R.T.L.; Sales, R.D.C.M. Moisture effect on the mechanical properties of additively manufactured continuous carbon fiber-reinforced Nylon-based thermoplastic. *Polym. Compos.* **2020**, *41*, 5227–5245. [CrossRef]
39. Giannakis, E.; Koidis, C.; Kyratsis, P.; Tzetzis, D. Static and fatigue properties of 3D printed continuous carbon fiber nylon composites. *Int. J. Mod. Manuf. Technol.* **2019**, *11*, 69–76.
40. Anton, H.; Florin, B.; Andrei-Daniel, V.; Daniel, V.; Daniela-Ioana, T.; Cătălin, A. Mechanical Characteristics Evaluation of a Single Ply and Multi-Ply Carbon Fiber-Reinforced Plastic Subjected to Tensile and Bending Loads. *Polymers* **2022**, *14*, 3213. [CrossRef]
41. Yoo, Y.; Spencer, M.W.; Paul, D.R. Morphology and mechanical properties of glass fiber reinforced Nylon 6 nanocomposites. *Polymer* **2011**, *52*, 180–190. [CrossRef]
42. Tomiak, F.; Schoeffel, A.; Rathberger, K.; Drummer, D. Expandable Graphite, Aluminum Diethylphospinate and Melamine Polyphosphate as Flame Retarding System in Glass Fiber-Reinforced PA6. *Polymers* **2022**, *14*, 1263. [CrossRef]
43. Etcheverry, M.; Barbosa, S.E. Glass fiber reinforced polypropylene mechanical properties enhancement by adhesion improvement. *Materials* **2012**, *5*, 1084–1113. [CrossRef] [PubMed]
44. Sodeifian, G.; Ghaseminejad, S.; Yousefi, A.A. Preparation of polypropylene/short glass fiber composite as Fused Deposition Modeling (FDM) filament. *Results Phys.* **2019**, *12*, 205–222. [CrossRef]
45. Salahuddin, B.; Mutlu, R.; Baigh, T.A.; Alghamdi, M.N.; Aziz, S. Self-Reinforced Nylon 6 Composite for Smart Vibration Damping. *Polymers* **2021**, *13*, 1235. [CrossRef] [PubMed]
46. Fiber Force Italy. Nylforce Carbon Fiber. Available online: https://marketplace.ultimaker.com/app/cura/materials/AliGhandour/fiberforce_NylonCarbon_2020 (accessed on 21 April 2022).
47. Fiber Force Italy. Nylforce Glass Fiber. Available online: https://marketplace.ultimaker.com/app/cura/materials/AliGhandour/Fiberforce_NylonGlass_2020 (accessed on 21 April 2022).
48. *ASTM D638-14*; Standard Test Method for Tensile Properties of Plastics. American Society of Testing and Materials: West Conshohocken, PA, USA, 2017. [CrossRef]
49. *ASTM D883-20b*; Standard Terminology Relating to Plastics. American Society of Testing and Materials: West Conshohocken, PA, USA, 2020. [CrossRef]
50. Genena, F.A.; Jamal, D.A.; Ahmed, W.K.; Almarzooqi, L.A.; Almazrouei, A.S.; Al-Naqbi, A.H. Implementing green solutions to recycle U.A.E. domestic waste: Aircraft composite materials. In Proceedings of the 2018 5th International Conference on Renewable Energy: Generation and Applications (I.C.R.E.G.A.), Al Ain, United Arab Emirates, 25–28 February 2018; pp. 30–33. [CrossRef]
51. Mansour, A.; Alabdouli, H.; Almehairi, A.R.; Alhammadi, M.; Alqaidy, H.; Ahmed, W.K.; Alnaqbi, A.H. Investigating the Compressive Strength of CFRP Pre-Preg Scrap from Aerospace Indu stries: Compression Molding. In Proceedings of the Advances in Science and Engineering Technology International Conferences (A.S.E.T.), Dubai, United Arab Emirates, 26 March–10 April 2019; pp. 1–6. [CrossRef]
52. Ahmed, W.K.; Alnaqbi, A.H.; Almazrouei, A.S.S.; Almarzooqi, L.A.A.M.; Al Jamal, D.; Genena, F.A.A. Method of Recycling Carbon Fiber Prepreg Waste. U.S. Patent No. 10,328,610B2, 25 June 2019.
53. Ahmed, W.K. Method of Recycling Carbon Fiber Prepreg Waste and Transparent Thermoplastic Waste. U.S. Patent No. 10,507,598B2, 17 December 2019.
54. Singh, B.; Kumar, K.; Chohan, J.C. Polymer matrix composites in 3D printing: A state of art review. *Mater. Today Proc.* **2020**, *33*, 1562–1567. [CrossRef]
55. Guessasma, S.; Belhabib, S.; Nouri, H. Effect of printing temperature on microstructure, thermal behavior and tensile properties of 3D printed Nylon using fused deposition modeling. *J. Appl. Polym. Sci.* **2020**, *138*, 50162. [CrossRef]

56. Gu, G.X.; Wettermark, S.; Buehler, M.J. Algorithm-driven design of fracture resistant composite materials realized through additive manufacturing. *Addit. Manuf.* **2017**, *17*, 47–54. [CrossRef]
57. FiberForce Italy. Nylforce Carbon Fiber Data Sheet. 2019. Available online: http://www.fiberforce.it/wp-content/uploads/2019/07/TDS_NY-CARBON_REV-2.1.pdf (accessed on 23 July 2022).
58. FiberForce Italy. Nylforce Glass Fiber Data Sheet. 2019. Available online: http://www.fiberforce.it/wp-content/uploads/2019/07/TDS_NY-GLASS_REV-2.0.pdf (accessed on 23 July 2022).
59. D20 Committee. *Guide for Determination of Thickness of Plastic Film Test Specimens*; ASTM International: West Conshohocken, PA, USA, 2013.
60. Mohammadizadeh, M.; Gupta, A.; Fidan, I. Mechanical benchmarking of additively manufactured continuous and short carbon fiber reinforced Nylon. *J. Compos. Mater.* **2021**, *55*, 3629–3638. [CrossRef]
61. Kumar Jain, P.A.; Sattar, S.; Mulqueen, D.; Pedrazzoli, D.; Kravchenko, S.G.; Kravchenko, O.G. Role of annealing and isostatic compaction on mechanical properties of 3D printed short glass fiber nylon composites. *Addit. Manuf.* **2022**, *51*, 102599. [CrossRef]
62. Nuruzzaman, D.M.; Asif Iqbal, A.K.M.; Oumer, A.N.; Ismail, N.M.; Basri, S. Experimental investigation on the mechanical properties of glass fiber reinforced Nylon. *Mater. Sci. Eng.* **2016**, *114*, 012118. [CrossRef]
63. Gensamer, M. Strength and Ductility. *Metallogr. Microstruct. Anal.* **2017**, *6*, 171–185. [CrossRef]
64. Dey, D.; Srinivas, D.; Panda, B.; Suraneni, P.; Sitharam, T.G. Use of industrial waste materials for 3D printing of sustainable concrete: A review. *J. Clean. Prod.* **2022**, *340*, 130749. [CrossRef]
65. Chong, S.; Yang, T.C.K.; Lee, K.C.; Chen, Y.F.; Juan, J.C.; Tiong, T.J.; Huang, C.M.; Pan, G.T. Evaluation of the physico-mechanical properties of activated-carbon enhanced recycled polyethylene/polypropylene 3D printing filament. *Sādhanā* **2020**, *45*, 57. [CrossRef]
66. Patti, A.; Cicala, G.; Acierno, D. Eco-sustainability of the textile production: Waste recovery and current recycling in the composites world. *Polymers* **2020**, *13*, 134. [CrossRef] [PubMed]
67. Rafiq, R.; Cai, D.; Jin, J.; Song, M. Increasing the toughness of nylon 12 by the incorporation of functionalized graphene. *Carbon* **2010**, *48*, 4309–4314. [CrossRef]
68. Pakkanen, J.; Manfredi, D.; Minetola, P.; Iuliano, L. About the use of recycled or biodegradable filaments for sustainability of 3D printing. In Proceedings of the International Conference on Sustainable Design and Manufacturing, Bologna, Italy, 26–28 April 2017; Springer: Cham, Switzerland, 2017; pp. 776–785.
69. Vidakis, N.; Petousis, M.; Tzounis, L.; Maniadi, A.; Velidakis, E.; Mountakis, N.; Kechagias, J.D. Sustainable additive manufacturing: Mechanical response of polyamide 12 over multiple recycling processes. *Materials* **2021**, *14*, 466. [CrossRef]
70. Saadatkhah, N.; Carillo Garcia, A.; Ackermann, S.; Leclerc, P.; Latifi, M.; Samih, S.; Patience, G.S.; Chaouki, J. Experimental methods in chemical engineering: Thermogravimetric analysis—TGA. *Can. J. Chem. Eng.* **2020**, *98*, 34–43. [CrossRef]
71. Liu, X.; Yu, W. Evaluating the thermal stability of high-performance fibers by TGA. *J. Appl. Polym. Sci.* **2006**, *99*, 937–944. [CrossRef]
72. Aljarrah, M.T.; Abdelal, N.R. Improvement of the mode I interlaminar fracture toughness of carbon fiber composite reinforced with electrospun nylon nanofiber. *Compos. Part B Eng.* **2019**, *165*, 379–385. [CrossRef]
73. Feng, N.; Wang, X.; Wu, D. Surface modification of recycled carbon fiber and its reinforcement effect on nylon 6 composites: Mechanical properties, morphology and crystallization behaviors. *Curr. Appl. Phys.* **2013**, *13*, 2038–2050. [CrossRef]
74. Prajapati, A.R.; Dave, H.K.; Raval, H.K. An Experimental Study on Mechanical, Thermal and Flame-Retardant Properties of 3D-Printed Glass-Fiber-Reinforced Polymer Composites. *J. Mater. Eng. Perform.* **2021**, *30*, 5266–5277. [CrossRef]
75. Mohamed, M.A.; Jaafar, J.; Ismail, A.F.; Othman, M.H.D.; Rahman, M.A. Fourier transform infrared (FTIR) spectroscopy. In *Membrane Characterization*; Elsevier: Amsterdam, The Netherlands, 2017; pp. 3–29. [CrossRef]
76. Petit, T.; Puskar, L. FTIR spectroscopy of nanodiamonds: Methods and interpretation. *Diam. Relat. Mater.* **2018**, *89*, 52–66. [CrossRef]
77. Charles, J.; Ramkumaar, G.R.; Azhagiri, S.; Gunasekaran, S. FTIR and Thermal Studies on Nylon-66 and 30% Glass Fibre Reinforced Nylon-66. *J. Chem.* **2009**, *6*, 909017. [CrossRef]
78. An, T.; Pant, B.; Kim, S.Y.; Park, M.; Park, S.J.; Kim, H.Y. Mechanical and optical properties of electrospun nylon-6, 6 nanofiber reinforced cyclic butylene terephthalate composites. *J. Ind. Eng. Chem.* **2017**, *55*, 35–39. [CrossRef]
79. Nadagouda, M.N.; Ginn, M.; Rastogi, V. A review of 3D printing techniques for environmental applications. *Curr. Opin. Chem. Eng.* **2020**, *28*, 173–178. [CrossRef]
80. Al-Mazrouei, N.; Ismail, A.; Ahmed, W.; Al-Marzouqi, A.H. ABS/Silicon Dioxide Micro Particulate Composite from 3D Printing Polymeric Waste. *Polymers* **2022**, *14*, 509. [CrossRef]